



BIULETYN WAT
VOL. L, NR 8 (2001)

Blue fluorescence in $\text{Li}_2\text{B}_4\text{O}_7$ glasses doped with rare-earths and transition metal ions

SŁAWOMIR M. KACZMAREK
MAREK GRINBERG**
KRZYSZTOF WIŚNIEWSKI*

CZESŁAW KOEPKE*
ANDRZEJ MAJCHROWSKI***
MARIUSZ CZUBA

Military University of Technology, Institute of Optoelectronics, 2 Kaliski Str.,
00-908 Warsaw, Poland

* Institute of Physics, N. Copernicus University, Grudzińska 5/7,
87-100 Toruń, Poland

** Institute of Experimental Physics, University of Gdańsk, Wita Stwosza 57,
80-952 Gdańsk, Poland

*** Military University of Technology, Institute of Physics, 2 Kaliski Str.,
00-908 Warsaw, Poland

Abstract. Absorption and emission spectra of Cr, Eu and Dy ions in $\text{Li}_2\text{B}_4\text{O}_7$ glasses melted in oxygen and hydrogen were measured for valency states and excited states analysis. It was stated that the presence of Cr^{6+} ion is limited by composition of the starting mixture and atmosphere of the melting and that this ion arises as Cr^{6+}O_4 complex. The 308 nm line excites the $\text{Li}_2\text{B}_4\text{O}_7:\text{Cr}$ glass within the highest absorption peak which can be ascribed to the following charge transfer transition: $\text{Cr}^{6+}\text{O}_4(3d^0 2p^6) \rightarrow \text{Cr}^{5+}\text{O}(3d^1 2p^5)$. Under gamma irradiation Cr^{6+}O_4 complex of $3d^0$ configuration can be disintegrated giving additional absorption bands of Cr^{3+} and may be Cr^{4+} centers at tetrahedral sites. One of these additional absorption bands may be (beside self-emission of the glass) responsible for 430 nm emission.

Keywords: crystallography, fluorescence crystals, $\text{Li}_2\text{B}_4\text{O}_7$ glass

Universal Decimal Classification: 548

1. Introduction

In the last four decades a great effort has been devoted to the study of glasses containing transition metal and rare-earth impurities¹⁻⁵. Glasses as laser hosts have advantages such as mass production at low cost and form fibers more easily than single crystals. The emission properties in the glasses are characterized by broader emission spectra, a radiation lifetime with a non-exponential decay law, a peculiar temperature dependence of the quantum efficiency⁶.

Lithium tetraborate ($\text{Li}_2\text{B}_4\text{O}_7$ or LBO) is a congruently melting compound with a melting point 917°C . Single crystals of this material are used as substrates for surface acoustic wave (SAW) devices. The material has cuts with temperature stability of acoustic wave velocity and relatively high electromechanical coupling coefficient for SAW. Polycrystals of $\text{Li}_2\text{B}_4\text{O}_7$ with some dopants find also applications in thermoluminescent personal dosimeters⁷.

Owing to small ionic radii of lithium and boron it is impossible to introduce dopants into $\text{Li}_2\text{B}_4\text{O}_7$ single crystals at high levels. Relatively high viscosity of molten lithium tetraborate, like other borates, is a source of serious problems during single crystals growth of this material. On the other hand this viscosity allows to obtain the material in a form of glass containing much higher amounts of dopants than in case of single crystals.

One of the most investigated impurity ions also in glasses is chromium, and the large number of review articles and papers testifies to the high level of interest in this field^{4, 5, 8}, even in connection with the development of lasers. Europium and dysprosium doped glasses exhibit wide application in gamma dosimetry and as scintillators.

In this paper we point out the possibility of hosting easily impurity ions: Cr, Eu, Dy in a $\text{Li}_2\text{B}_4\text{O}_7$ glassy matrix. The purpose of this work is also to investigate possible valency states and excited states of Cr, Eu and Dy ions in $\text{Li}_2\text{B}_4\text{O}_7$ glasses.

2. Experimental procedure

2.1. Glass preparation

The synthesis of lithium tetraborate was carried out from lithium carbonate Li_2CO_3 , and boric oxide H_3BO_3 (Merck, extra pure) in platinum crucibles in air. After reaction of starting materials at 950°C the obtained compound was overheated to 1150°C to remove traces of water and carbon dioxide, which were present in the melt. Because of B_2O_3 losses, due to

evaporation, 1 mol% surplus of H_3BO_3 was added to the starting composition. After rapid cooling below 550°C the melt formed glass which did not show any tendency to crystallise. Prolonged heating of obtained glass at temperatures higher than 600°C led to its crystallisation and subsequent formation of polycrystalline material. Cr_2O_3 was dissolved in lithium tetraborate at the level of 0.13 mol% and 2.5 mol%. The addition of chromium oxide, Cr_2O_3 , caused green coloration of the glass. The glasses were obtained in oxidizing atmosphere.

Almost completely transparent $\text{Li}_2\text{B}_4\text{O}_7$ glasses doped with Eu, Dy were obtained in oxidizing and reducing atmosphere of hydrogen.

The following $\text{Li}_2\text{B}_4\text{O}_7$ glasses were obtained: doped with Cr (0.13 wt. % and 2.5 wt. %), and Eu, Dy (2wt.%, 2wt.%).

2.2. Absorption and photoluminescence measurements

The samples were polished to the thickness of about 1 mm. They were also irradiated by gamma photons immediately after growth process. The ^{60}Co gamma source with a power of 1.5 Gy/sec was used. Optical transmission was measured before and after γ treatment using LAMBDA-900 Perkin-Elmer spectrophotometer in UV-VIS range and FTIR-1725 in the IR range. Additional absorption was calculated according to the formula:

$$\Delta K(\lambda) = (1/d) \ln(T_1/T_2) \quad (1)$$

where K is the absorption, λ is the wavelength, d is the sample thickness and T_1 and T_2 are transmissions of the sample before and after a treatment, respectively.

Photoluminescence (PL) was recorded using Perkin-Elmer spectrofluorimeter from 200-900 nm and He-Ne laser excitation of 630 nm.

2.3. Excited state absorption investigations

The excited state absorption (ESA) spectra were measured using a setup which utilized a RD-EXC-150/25 XeCl excimer laser (308 nm) as a source of excitation, a Hamamatsu Xe flash lamp as a source of probe beam and ORIEL InstaSpec II photodiode array detector coupled to MultiSpec 1/8 m spectrograph in the detection branch. The setup operated in pulsed regime and transverse geometry (like in ⁹).

3. Results and discussion

3.1 Absorption and photoluminescence

3.1.1 Absorption and the additional absorption measurements

Figs 1-5 show absorption spectra of representative samples obtained at 300K.

In the case of pure $\text{Li}_2\text{B}_4\text{O}_7$ glass (Fig. 1, curve 1) the range of transparency origins at 190 nm (fundamental absorption edge - FAE) and ends at about 2700 nm (lattice absorption). Curve 2 shows absorption of this glass after γ -irradiation with a dose of $5 \cdot 10^4$ Gy.

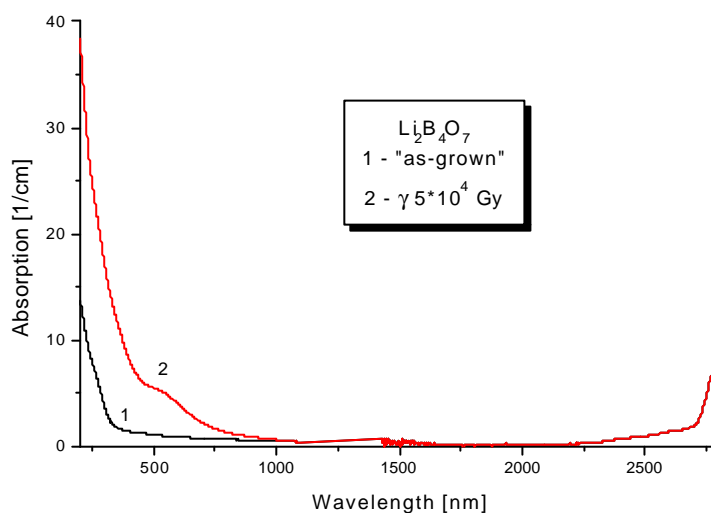


Fig. 1. Absorption of $\text{Li}_2\text{B}_4\text{O}_7$ glass before (1) and after (2) γ -irradiation with a dose of $5 \cdot 10^4$ Gy

In the 0.15wt% chromium doped $\text{Li}_2\text{B}_4\text{O}_7$ glass (Fig. 2a and 2b, curve 1) we observe Cr^{3+} and Cr^{6+} ions spectra. FAE of the glass is equal to 245 nm and lattice absorption origin at 2700 nm. The Cr^{3+} ion has two absorption bands centered at about 430 and 614 nm due to d-d transition: the former was attributed to the spin-allowed but parity forbidden ${}^4\text{A}_2\text{-}{}^4\text{T}_1$ transition and the latter to the spin-allowed but parity-forbidden ${}^4\text{A}_2\text{-}{}^4\text{T}_2$ transition. The Cr^{6+} ion has strong absorption band centered at 358 nm and a weak one at 318 nm. It seems that these bands refer to Cr^{6+}O_4 complex of $3d^0$ configuration rather than to Cr^{6+} ion⁵. Curve 2 shows absorption of the glass after 10^5 Gy γ -rays while curve 3 the additional absorption. There are seen at least two bands in the additional absorption centered at about 297

and 450 nm. Curve 4 in Fig. 2b shows the absorption of highly doped with Cr (2.5wt.%) $\text{Li}_2\text{B}_4\text{O}_7$ glass. One can see that in case of high doping only 614 nm band due to $^4\text{A}_2\text{-}^4\text{T}_2$ transition in Cr^{3+} ions is present.

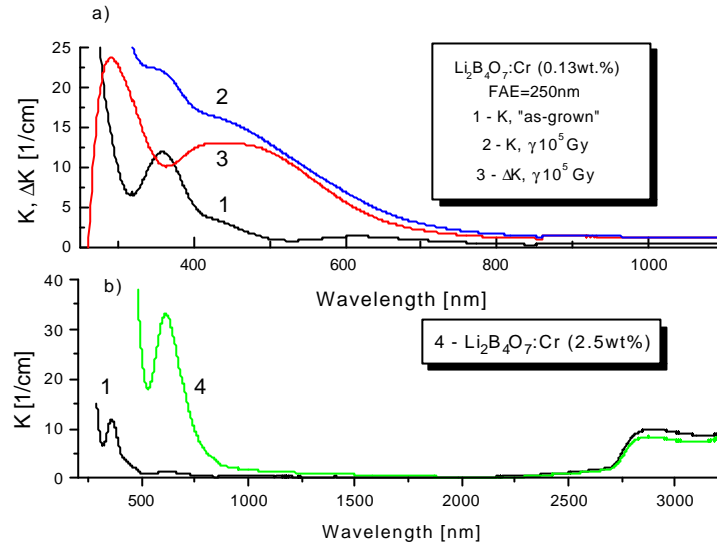


Fig. 2. Absorption before (1) and after γ -irradiation (2) and additional absorption (3) of $\text{Li}_2\text{B}_4\text{O}_7:\text{Cr}$ (0.13wt.%) glass, and absorption of $\text{Li}_2\text{B}_4\text{O}_7:\text{Cr}$ (2.5wt.%) glass (4)

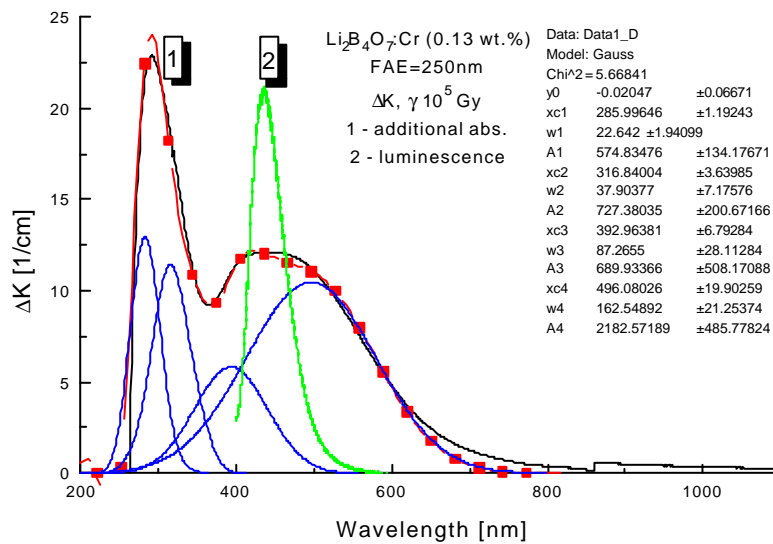


Fig. 3. Gauss distribution of the additional absorption in $\gamma 10^5$ Gy irradiated $\text{Li}_2\text{B}_4\text{O}_7:\text{Cr}$ (0.13wt.%) glass (1) and photoluminescence of the glass (2) excited with 260 nm

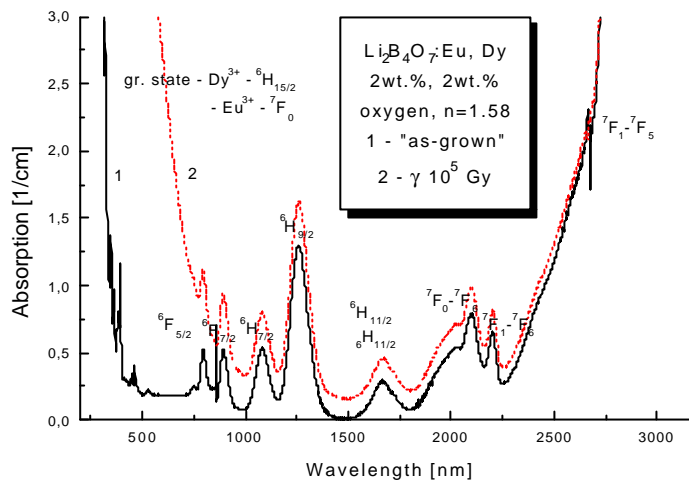


Fig. 4. The absorption of $\text{Li}_2\text{B}_4\text{O}_7:\text{Eu, Dy}$ (2wt.%, 2wt.%) glass obtained in oxygen atmosphere at 300K before (1) and after (2) γ -irradiation with a dose of 10^5 Gy

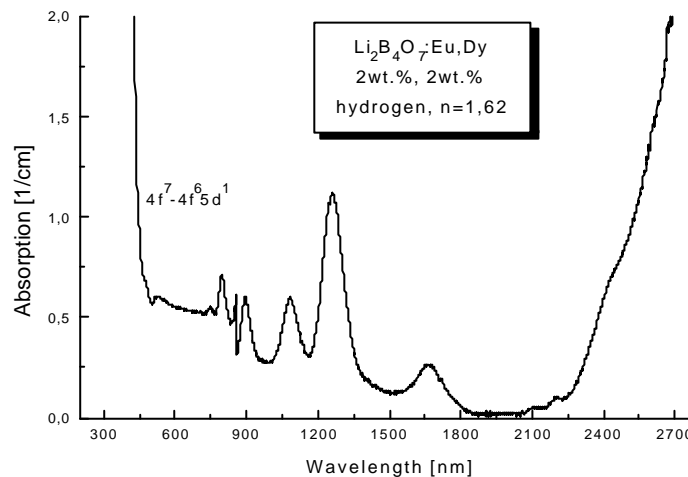


Fig. 5. Absorption of $\text{Li}_2\text{B}_4\text{O}_7:\text{Eu, Dy}$ (2wt.%, 2wt.%) glass obtained in hydrogen atmosphere

Detailed analysis using the fitting with Gauss curves have shown that there are at least four bands in the additional absorption centered at about 285 nm, 316 nm, 392 nm and 496 nm (Fig. 3) which are responsible for 297 nm and 450 nm additional absorptions. Three of them seem correspond to previously described color centers in $\text{Li}_2\text{B}_4\text{O}_7$ glasses. Fourth, at about 392 nm, seems to be responsible for 430 nm emission observed after 260 nm excitation. This broad-band 450 nm additional absorption may be due to ${}^4\text{A}_2-{}^4\text{T}_2$, ${}^4\text{T}_1$ transitions in Cr^{3+} and/or ${}^3\text{A}_2-{}^3\text{T}_2$, ${}^3\text{T}_1-{}^3\text{T}_2$ transitions in Cr^{4+} ¹⁰. Parameters of the fitting are listed in a table inside the figure.

Fig. 4 presents the absorption (1) from two ground states: $Dy^{3+} - {}^6H_{15/2}$ and $Eu^{3+} - {}^7F_0$ of $Li_2B_4O_7:Eu, Dy$ (2wt.%, 2wt.%) glass. As one can see FAE in this case is equal to 270 nm. Refraction coefficient is equal to 1.58. Curve 2 show the absorption after γ -irradiation with a dose of 10^5 Gy. Fig. 5 shows the absorption of Dy^{3+} from ${}^6H_{15/2}$ ground state and Eu^{2+} transitions $4f^7-4f^65d^1$ ¹¹. FAE is equal to about 355 nm and refraction coefficient 1.62.

3.1.2. Photoluminescence measurements

Fig. 6 presents photoluminescence of $Li_2B_4O_7:Cr$ glasses excited with 630 nm He-Ne laser. As one can see gamma irradiation leads to the increase in Cr^{3+} PL intensity.

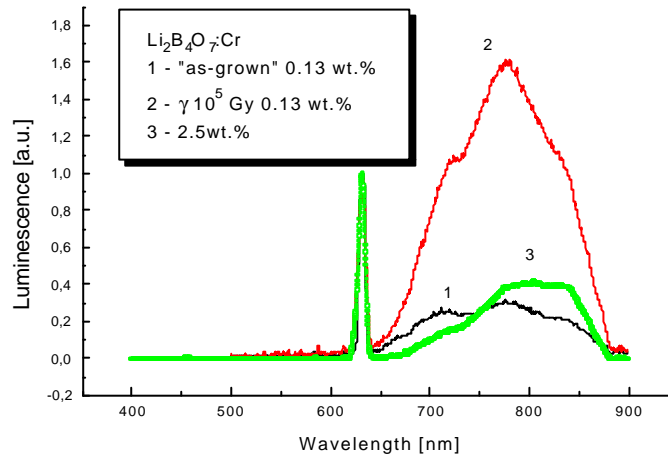


Fig. 6. Photoluminescence of $Li_2B_4O_7:Cr$ glasses excited by 630 nm He-Ne laser: 0.13wt.%Cr “as-grown” (1), 0.13wt.%Cr γ -irradiated with a dose of 10^5 Gy and 2.5wt.%Cr (3)

Fig. 7 shows excitation-emission spectra of $Li_2B_4O_7:Cr$ (0.13wt.%) glass after γ -exposure with a dose of 10^5 Gy (a) and emission from $Li_2B_4O_7:Cr$ (2.5wt.%) glass (b) under 270 nm excitation. As one can see emission at 430 nm is due to excitation at 362 nm and 385 nm. This same type of emission is observed also in case of high doping of the glass with Cr (Fig. 7b). It may be possible that the latter emission is connected also with the self-emission of the glass.

The shape of emission spectrum from $Li_2B_4O_7:Eu, Dy$ (2wt.%, 2wt.%) glass strongly depend on the type of growth atmosphere. Fig. 8 shows characteristic emissions for the two basic cases of the obtaining of the glasses: oxidizing (a) and reducing (b) atmospheres ¹¹.

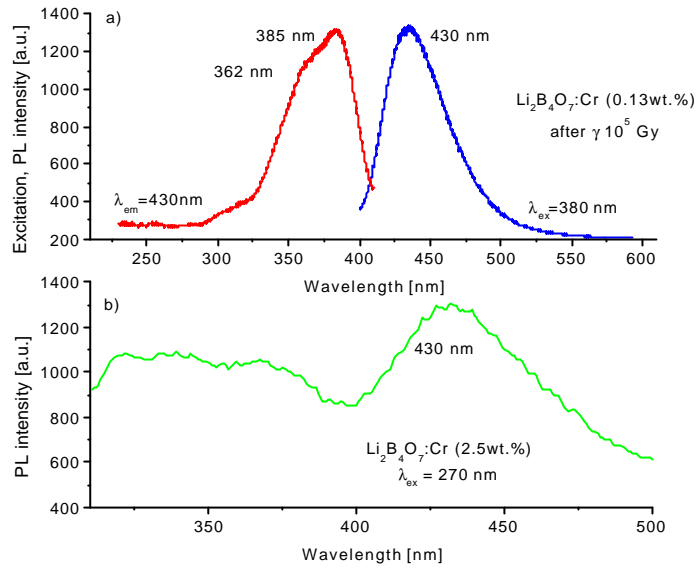


Fig. 7. Excitation-emission spectra of $\text{Li}_2\text{B}_4\text{O}_7:\text{Cr}$ (0.13wt.%) glass after γ -exposure with a dose of 10^5 Gy (a) and emission from $\text{Li}_2\text{B}_4\text{O}_7:\text{Cr}$ (2.5wt.%) glass (b) under 270 nm excitation

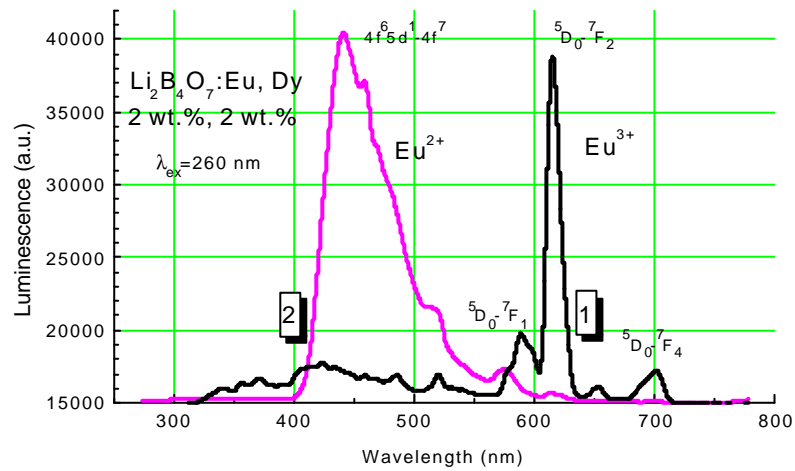


Fig. 8. Emission spectra of $\text{Li}_2\text{B}_4\text{O}_7:\text{Eu}, \text{Dy}$ (2wt.%, 2wt.%) glasses obtained in oxidizing (1) and reducing (2) atmosphere

3.1.3. Discussion

As one can see in Fig. 1 the absorption spectrum of pure $\text{Li}_2\text{B}_4\text{O}_7$ glass shows a transmission range larger than of other glasses¹. The relevant feature of the glass, as it take place also in case of other glasses, is its high susceptibility to gamma irradiation. Wide, almost non-structural additional absorption in the UV-VIS and NIR of the absorption spectrum (190-1000 nm) is seen with weakly distinguished bands centered at about: 250 nm, 360 nm and 530 nm.

As one can see from Fig. 2 some changes under gamma radiation may be positive one. Our experimental data cannot be interpreted in terms of Cr^{3+} alone, but have to be analyzed in view of the coexistence of Cr ions of different valences. Low chromium doped $\text{Li}_2\text{B}_4\text{O}_7$ glass shows presence of Cr^{3+} and Cr^{6+} ions. The former like exist octahedrally coordinated while the latter tetrahedrally coordinated. The former give well known emission, which is clearly seen in Fig. 6 for $\lambda_{\text{ex}}=630$ nm of He-Ne laser. The latter does not give emission because Cr^{6+}O_4 complex of $3d^0$ configuration seem to be responsible for the 318 and 358 nm absorption. But under gamma irradiation with a dose of 10^5 Gy Cr^{6+}O_4 complex disintegrates giving additional absorption connected with the above mentioned, specific for $\text{Li}_2\text{B}_4\text{O}_7$ color centers and 392 nm band which may be attributed to ${}^3\text{A}_2\text{-}{}^3\text{T}_2$, ${}^3\text{T}_1\text{-}{}^3\text{T}_2$ transitions in Cr^{4+} and/or ${}^4\text{A}_2\text{-}{}^4\text{T}_2$, ${}^4\text{T}_1$ transitions in Cr^{3+} (Fig. 3). Emission spectrum of the gamma irradiated glass reveal an increase in PL intensity of Cr^{3+} ions (Fig. 6), while excitation-emission spectra presented in Fig. 7a suggests presence of other luminescence center. It was previously reported that the Cr^{4+} ion exists in aluminate based glasses¹². The mechanism of forming Cr^{4+} ions was detail discussed in⁵ based on point defects in the glasses. It was stated that Cr^{4+} is observed only in glasses in which oxygen excess defects such as super oxide ion radicals and peroxy linkages are observed. It is possible that in our case Cr^{6+}O_4 complex disintegrates simultaneously to Cr^{4+} and Cr^{3+} . But it demand more and detailed investigations.

Highly doped with chromium $\text{Li}_2\text{B}_4\text{O}_7$ glasses show presence only ${}^4\text{A}_2\text{-}{}^4\text{T}_2$ absorption band (Fig. 2b) although 430 nm emission is also observed (Fig. 7b). Analyzing low and high doping in case of $\text{Li}_2\text{B}_4\text{O}_7$ glass one can state that there exists compositional dependence of the valency states of Cr ions in the glasses. In⁵ it was stated that the contents of Cr^{3+} and Cr^{6+} vary systematically with basicity in the silicate and borate glasses.

Europium¹¹ and dysprosium co-doping characterizes dependency of Eu valence on growth atmosphere. As one can see in Fig. 4 absorption of $\text{Li}_2\text{B}_4\text{O}_7\text{:Eu}$, Dy glass obtained in oxidizing atmosphere shows many transitions from ground state of Dy^{3+} (${}^6\text{H}_{15/2}$) and ground state of Eu^{3+} (${}^7\text{F}_0$) to higher states. Gamma irradiation does not change a valence of the impurities, but leads to strong additional absorption in the range 270-1000

nm. In case of $\text{Li}_2\text{B}_4\text{O}_7:\text{Eu}$, Dy glass obtained in reducing atmosphere of hydrogen (Fig. 5) well known transitions of Dy^{3+} ions are seen in the absorption spectrum and the new one $4f^7-4f^65d^1$ of Eu^{2+} ions. Emission of both types Eu ions is clearly seen in Fig. 8. As it follows from emission measurements both types of Eu ions exists in both types of the obtained glasses, but one of them dominates giving characteristic emission.

3.2 Excited state absorption measurements of Cr:LBO (0.15 wt.%) glass

The ESA spectrum of the Cr:LBO (0.15wt.%) glass sample is presented in figure 9. As it is seen, there is no chance to fit this ESA spectrum by a single Gaussian function, whereas two Gaussians {one relatively narrow (2800 cm^{-1}) and another much broader (8200 cm^{-1})} fit the spectrum perfectly. This strongly suggests that the observed ESA under UV excitation consists of transitions to two distinctly defined excited states.

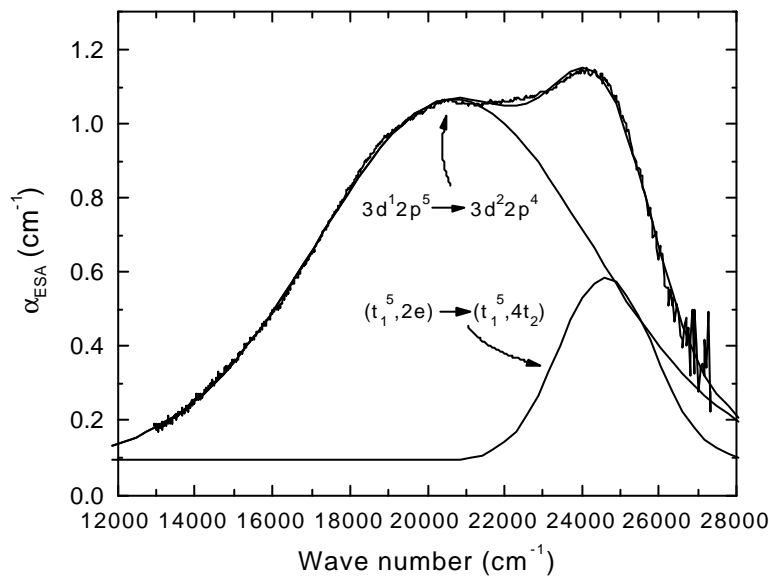


Fig. 9 Experimental ESA spectrum obtained for 308 nm excitation, fit by two Gaussians, and assignation of the contributing ESA bands.

The single configuration coordinate (SCC) diagram can be used to reproduce a characteristic ESA spectrum comparable to that obtained with 308 nm excitation (figure 9). To achieve this, certain assumption has to be made, namely - the existence of additional excited electronic manifold, strongly coupled to the lattice, not detectable in the ground state absorption (GSA) spectrum. Such a state can be related to the $3d^2 2p^4$ electronic configuration of the central ion - ligand system. The $3d^2 2p^4$ excited

Table I

Parameters used to creation of the SCC diagram explaining the ESA spectra shown in Fig. A. \mathbf{k} is the elastic constant and \mathbf{G} are the half-widths corresponding to the respective relaxation energies $s_{\hbar\omega}$

Parameter	Energy (cm ⁻¹)
\mathbf{k}	8000
$\hbar\omega$	250
$\hbar\omega'$	400
kT	200
CT_1	27933
CT_2	42500
\mathbf{G}_1	4450
\mathbf{G}_2	8200
\mathbf{G}_3	2800
ESA_1	20520
ESA_2	24600

electronic configuration origins from the consecutive excitation of two electrons from the valence band (made mostly of ligands orbitals) to the d orbitals of the central ion. The resulting SCC diagram calculated using the parameters given in Table I is presented in Fig. 10 together with definitions of energies taken from the experiment. It shows two positions of the state $|3\rangle$ ($3d^22p^4$) (dashed and solid) corresponding to two qualitatively different situations described in the caption.

Considering the nature of the electronic configurations which the SCC diagram is constructed from, one should remember that Cr^{6+}O_4 centre is a typical d^0 complex (of approximated T_d symmetry). Then it is possible to write formally the electronic configuration of the central ion-ligand system as $3d^02p^6$ ¹³. The exemplary molecular orbital diagram for tetrahedral MX_4 complex [14-16] is illustrated in figure 11. It is noted that the highest occupied bonding orbital t_1 of the ground state of such a complex is composed exclusively from ligand p_π orbitals. The higher, nonbonding molecular orbital $2e$ is of d type and consists mostly d orbital of the central ion, whereas the next antibonding orbital $4t_2$ is a typical mixed orbital consisting d orbital of the central ion but also p_σ orbitals of the ligands.

This is why the parabola corresponding to $(t_1^5, 4t_2)$ symmetry is shifted with respect to the $(t_1^5, 2e)$ parabola (different charge distributions and consequently different couplings to the lattice). The ground state

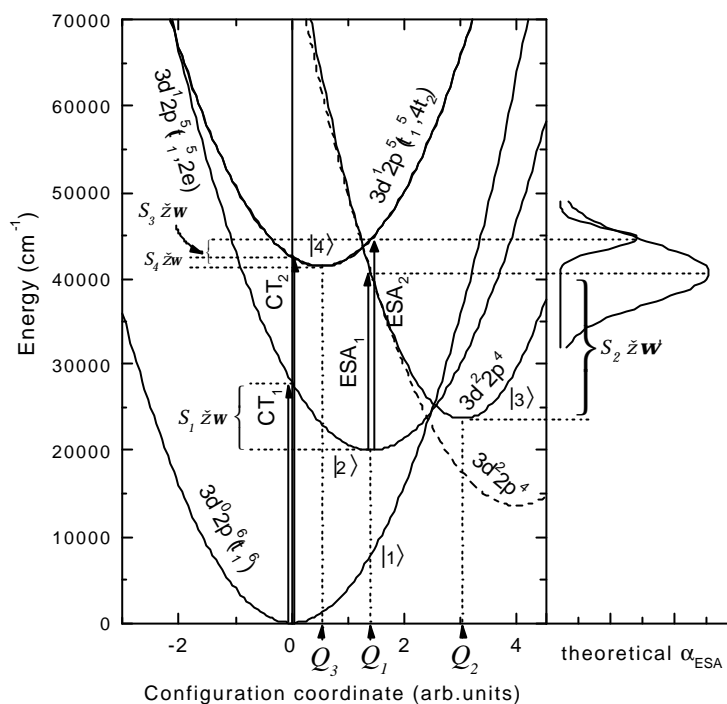


Fig. 10 SCC diagram quantitatively reproducing the ESA spectrum obtained with 308 nm excitation. Right side of the figure shows two Gaussian ESA spectra (of the widths corresponding to the respective relaxation energies) whose composition fits the experiment. The dashed parabola corresponds to the $3d^22p^4$ state of linear coupling to the lattice i.e. with the same phonon energy as all remaining states ($\hbar\omega = 250 \text{ cm}^{-1}$). The solid parabola of the $3d^22p^4$ state corresponds to the different phonon energy $\hbar\omega = 400 \text{ cm}^{-1}$

absorption (CT_1) is due to one of the t_1 electrons, making a transition to the $2e$ orbital and leaving a hole in the bonds. Because the transition occurs practically from the ligands to central-ion d orbital, this is what is usually called “charge transfer transition”, resulting in a distinct charge redistribution. This is consistent with the right-hand shift of the first excited state parabola. There is also another absorption, CT_2 , which is involved with a transition of one of the t_1 electrons to $4t_2$ orbital with suitably smaller charge redistribution. Thus the CT transition transforms the centre $Cr^{6+}O_4$ to $Cr^{5+}O^-$ centre of $3d^12p^5$ configuration [12]. The larger energy ESA transition (ESA_2) is from d-type $2e$ to more diffused $4t_2$ orbital of mixed d-p type. This is also charge redistribution (simplifying: from central ion back to ligands) which results in the $(t_1^5, 4t_2)$ parabola shifted back in respect to shift of the $(t_1^5, 2e)$ parabola, almost to the same position as the ground state parabola. The smaller energy ESA transition (ESA_1) occurs also from the state of $(t_1^5, 2e)$ configuration but to the state of quite different electronic configuration, namely $3d^22p^4$. The model discussed above and the goodness of the fit to experimental data suggested the manifold involved is of the $3d^22p^4$ electronic configuration.

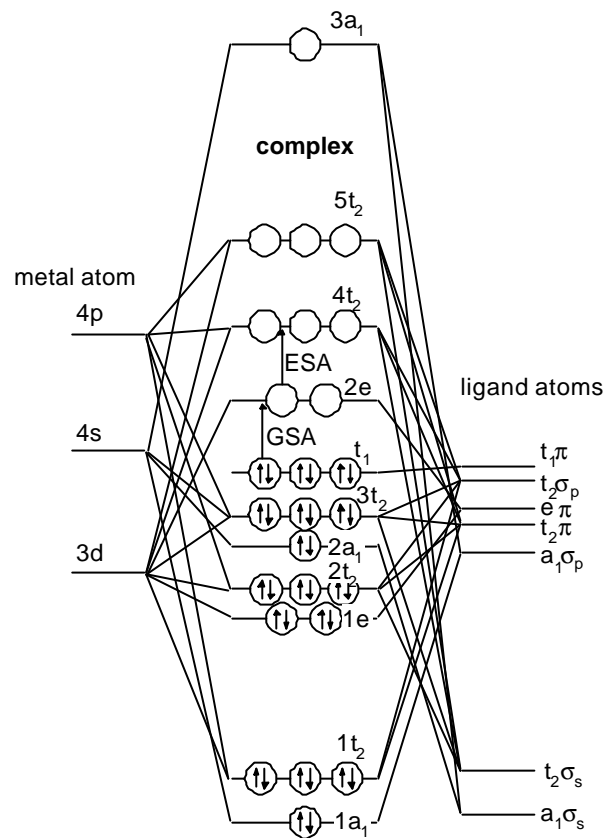


Fig. 11 Schematic molecular orbital energy level diagram for MX_4 type complexes (after [e], where the case of MnO_4^- complex was considered). The GSA and ESA transitions are indicated

If we compare ESA spectrum (Fig. 9) and emission spectrum of pure glass than it can be seen that self-emission of $Li_2B_4O_7$ glass coincide with short-wavelength ESA band. The reason of this phenomenon demand more investigations.

4. Conclusions

It was shown that in case of $Li_2B_4O_7$ glasses it is possible high doping with transition metal and rare-earth element impurities. Obtained compounds are good optical quality, giving clear luminescence especially for Cr^{3+} and Eu^{3+} and Eu^{2+} ions.

It was stated that the presence of Cr^{6+} ion is limited by composition of the starting mixture and atmosphere of the melting (oxidizing). Independently on the above factors in all the glasses (high and low doped with Cr) there were present Cr^{3+} ions. The 308 nm line excites the

$\text{Li}_2\text{B}_4\text{O}_7:\text{Cr}$ (0.13 wt.%) glass within the highest absorption peak which can be ascribed to the following charge transfer transition: $\text{Cr}^{6+}\text{O}_4(3d^02p^6)\rightarrow\text{Cr}^{5+}\text{O}^-(3d^12p^5)$. Under gamma irradiation Cr^{6+}O_4 complex of $3d^0$ configuration can be disintegrated giving additional absorption band of Cr^{3+} and may be Cr^{4+} ions. There arises luminescence centered at about 430 nm that may be also connected with self-emission of the glass. Gamma irradiation of $\text{Li}_2\text{B}_4\text{O}_7$ glass leads to arising of strong additional absorption in the range of 190-1000 nm with weakly distinguished bands peaked at about: 250 nm, 360 nm and 530 nm.

The content and optical characteristics of Eu^{2+} and Eu^{3+} doped $\text{Li}_2\text{B}_4\text{O}_7$ glasses are dependent of the growth atmosphere.

This work was supported by the State Committee for Scientific Research (KBN) under grants numbers: 2 P03B 117 16 and 2 P03B 063 16 and by Gdańsk University Grant no 5200-5-0299-0.

Received January 16, 2001; revised February 21, 2001

REFERENCES

1. H.L. Smith and A. Cohen, *J. Phys. Chem. Glasses* **4**, p. 173, 1963.
2. P.C. Schultz, *J. Am. Ceram. Soc.* **57**, p. 307, 1974.
3. A. Lempicki, L. Andrews, S.J. Nettel, B.C. McCollum and E.I. Solomon, *Phys. Rev. Lett.* **44**, p. 1234, 1980.
4. M. Casalboni, V. Ciafardonne, G. Giuli, B. Izzi, E. Paris and P. Proposito, "An optical study of silicate glass containing Cr^{3+} and Cr^{6+} ions", *J. Phys.: Condens. Matter* **8**, pp. 9059-9069, 1996.
5. T. Murata, M. Torisaka, H. Takebe and K. Morinaga, "Compositional dependence of the valency state of Cr ions in oxide glasses", *J. Non-Cryst. Solids* **220**, pp. 139-146, 1997.
6. M. Yamaga, B. Henderson, K.P. O'Donnell and Y. Gao, *Phys. Rev. B* **44**, p. 4853, 1991.
7. A. Majchrowski, "Thermoluminescence in ionising radiation dosimetry", *Proc. SPIE* **2373**, pp. 397-400, 1995.
8. F. Rasheed, K.P. O'Donnell, B. Henderson and D. Hollis, "Disorder and the optical spectroscopy of Cr^{3+} -doped glasses: II. Glasses with high and low ligand fields", *J. Phys.: Condens. Matter* **3**, p. 3825, 1991.
9. Cz. Koepke, A. J. Wojtowicz, and A. Lempicki, "Excited-state absorption in excimer-pumped CaWO_4 crystals", *J. Luminescence* **54**, p. 345, 1993.
10. N.A. Kulagin, W.A. Sandulenko, "Ab initio theory of electronic centers of doped crystals. Chromium ions in oxide compounds", *Fiz. Tw. Tela*, **31**(1), pp. 243-249, 1989.

11. W. Chen, J.O. Malm, V. Zwiller, Y. Huang, S. Liu, R. Wallenberg, J.O. Bovin and L. Samuelson, "Energy structure and fluorescence of Eu^{2+} in ZnS:Eu nanoparticles", *Phys. Rev. B*, **61**(16), p. 11021, 2000
12. X. Wu, S. Huang, U. Hommerich, W.M. Yen, B.G. Aitken and M. Newhouse, *Chem. Phys. Lett.* **233**, p. 28, 1995.
13. H. Yuan, W. Jia, D. Cohen, W. M. Yen, and B. G. Aitken, "Optical spectroscopy of pentavalent chromium ions in glass", *Mat. Res. Soc. Symp. Proc.* **455**, p. 483, 1997.
14. C. J. Ballhausen and H. B. Gray, *Molecular Orbital Theory* (W.A. Benjamin, Inc.) New York, Amsterdam 1964, pp 123-128
15. M. Karplus and R. N. Porter, *Atoms and Molecules; An Introduction for Students of Physical Chemistry* (W.A. Benjamin, New York 1970)
16. B. N. Figgis , *Introduction to Ligand Fields* (Interscience, Wiley, New York 1966) pp. 196-200